International Journal of Environmental Science and Technology (2019) 16:2359–2372
https://doi.org/10.1007/s13762-018-1678-y

ORIGINAL PAPER

Green synthesis of nanostructured SiCs by using natural biopolymers (guar, tragacanth, Arabic, and xanthan gums) for oxidative desulfurization of model fuel

E. Khomand[1] · M. Afsharpour[1]

Received: 17 May 2017 / Revised: 3 February 2018 / Accepted: 2 May 2018 / Published online: 16 May 2018

Abstract
Mesoporous SiC ceramics were prepared using different natural biopolymers (guar, tragacanth, Arabic, and xanthan gum) as both template and carbon sources. Natural biopolymers are safe, biocompatible, and inexpensive materials that can be green candidates for carbon sources. Low-temperature magnesiothermic technique was used to form porous silicon carbide. In this study, tetraethylorthosilicate was prepared by sol–gel method and used as silica precursor. The mixture of silica and carbon sources was carbonized under argon atmosphere at 750 °C, and then, the reaction continued by adding magnesium powder at 700 °C. Products were characterized using SEM, BET/BJH, XRD, FTIR, and Raman spectroscopy. The produced SiC materials showed mesoporous structures with high surface area and identical structures related to their carbon precursors. The results suggest that the natural gums can be potentially used as carbon templates in controlled formation of nanostructures. Also the synthesized silicon carbide nanostructures were used as catalyst supports in oxidative desulfurization of a model fuel. For this purpose, MoO_3 was immobilized on the surface of SiC supports by using peroxo molybdenum complex. Such excellent catalytic performance was attributed in the presence of silicon carbide (99, 98, 94, and 93% conversion for SiCs produced from Arabic, xanthan, guar, and tragacanth, respectively).

Responsibility editor: M. Abbaspour

✉ M. Afsharpour
afsharpour@ccerci.ac.ir

[1] Inorganic Department, Chemistry & Chemical Engineering Research Center of Iran, Tehran 14335-186, Iran

Graphical Abstract

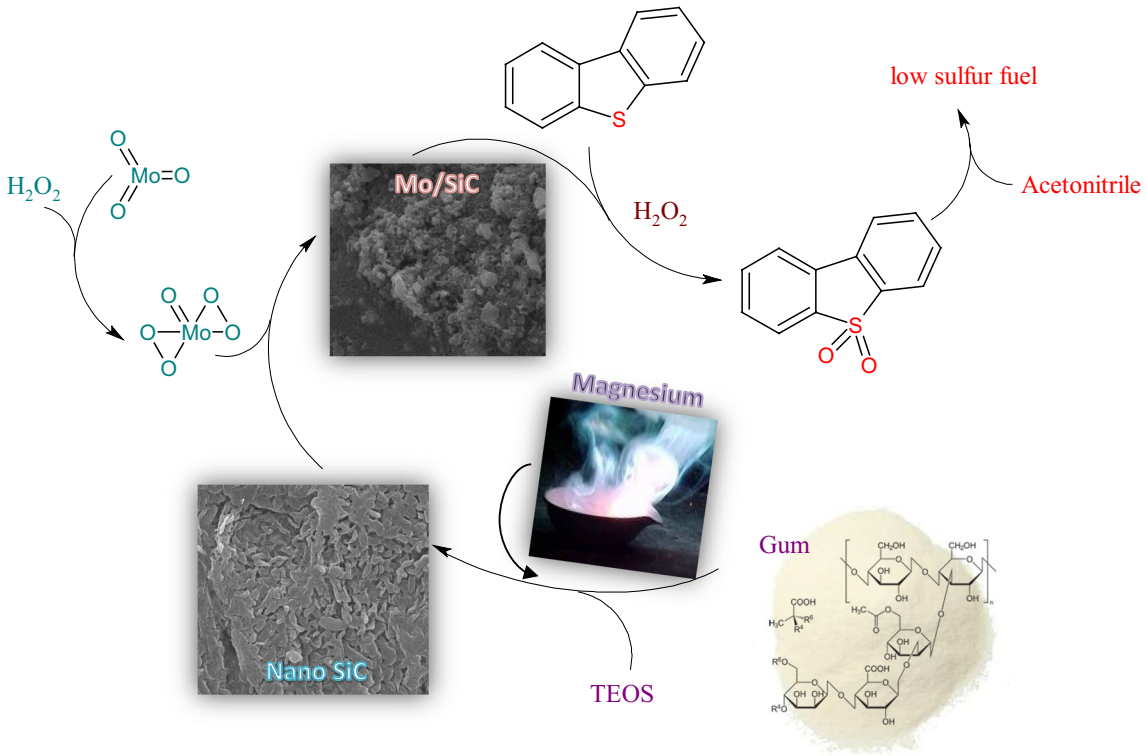

Keywords Green · Oxidative desulfurization · Natural gum · Silicon carbide

Introduction

Silicon carbide materials have attracted attention due to their specific properties such as semiconducting properties, good mechanical strength and thermal conductivity, chemical inertness, and excellent thermal shock resistance (Yang et al. 2005; Aristov et al. 2010). Compared to SiC bulk, nanostructured SiCs possess superior electrical, optical, and mechanical properties and are introduced as a good material for many applications such as catalyst support, drug delivery, and hydrogen storage (Ledoux and Pham-Huu 2001; Mélinon et al. 2007). Also, it is widely used for high-power electrical and optical devices (Wright et al. 2008; Eddy and Gaskill 2009).

These materials can be synthesized by different methods, including high-temperature pyrolysis of carbon/siloxane polymer, carbothermal reduction of silica, and grinding of silicon carbide stones in solid-phase reactions at high temperatures (Dasog et al. 2011; Henderson et al. 2009). These methods have some disadvantages including high-temperature synthesis method, not environmentally friendly, and expensive raw precursors (Rao et al. 2012; Magnani et al. 2014). In addition, these methods can not able to control the morphology of nanostructured materials due to the high-temperature reaction methods (Dasog et al. 2013). Magnesiothermic method is a good method, which makes nanoparticles at lower temperature to produce nanomaterial well. In this method, SiC has been produced by using magnesium powder that has a high thermic effect in a low-temperature solid-phase reaction (Dasog et al. 2013; Zhao et al. 2011; Jiang et al. 2013).

In this study, besides the use of this method which allowed to control the morphology and production of porous materials, we selected the cost-effective and accessible bio-carbon precursors. In general, porous materials have been made using surfactants or polymers as the templates. Template technique is used to control the structural properties such as surface area, internal porosity, and external shape (Davis et al. 2001). But, many surfactants are toxic for animals, humans, and ecosystems and may increase propagation of environmental pollution (Zhao et al. 2000; Sanchez et al. 2005; Wen et al. 2013). Most of polymers that are used as templates have petrochemical structure and expensive and most often are not suitable for biological applications (Lewis, 1992). These problems can be solved by using natural materials as green templates

(Selby and Wynne, 1973). Natural biopolymers are inexpensive, nontoxic, and environmentally friendly materials that can be selected as carbon templates. Among these biopolymers, polysaccharides have different molecular weights and chemical compounds with a large reactive groups that make them different in structure and properties (Prabaharan and Jayakumar 2009; Jayakumar et al. 2008). Moreover, natural biopolymers have infinite structures. Due to these characteristics, tragacanth, guar, xanthan, and Arabic gums with cellulose-like backbone were selected as suitable templates for the synthesis of nanostructured silicon carbide.

The aim of this work was the synthesis of porous materials with high surface area that can be used as catalyst supports (Daşdelen et al. 2017; Sen et al. 2017; Yildiz et al. 2017) Oxidative desulfurization is considered to be one promising method for the deep desulfurization of fuel oil. In this method, most of the sulfur compounds are removed under mild condition (Campos-Martin et al. 2010; Mjalli et al. 2014). Among much kind of catalysts, the supported molybdenum catalysts are active and widely used for oxidative desulfurization (ODS) (Chica et al. 2006; He et al. 2008; Prasad et al. 2008). Alumina (Tian et al. 2015; Garcia-Gutierrez et al. 2008), silica (De Filippis and Scarsella 2008), and activated carbon (Haw et al. 2010) are usually used as catalyst supports. In previous work, we reported the catalytic properties of SiC/MoC_2 composites in the ODS process (Afsharpour and Rostami Amraee 2017). The intrinsic structure of SiC and its defects made it good material in catalytic applications. The main advantages of using these bio-SiCs as catalyst supports include low synthesis temperature, inexpensive, and environmentally friendly raw material precursors, and excellent catalytic properties. In this work, a combined extraction–oxidation system for ODS process

Table 1 The optimum conditions for the synthesis of nanostructures of silicon carbide

Gums	Gum weight (g)	Volume of solvent (ml)	TEOS (ml)	Magnesium weight (g)	Ultrasonic (min)	Volume of acid (ml)
Arabic gum	10	40	8	1.0969	15	1.3
Tragacanth	3	50	5	1.0969	15	1
Guar	2	60	4.5	0.9872	15	1.1
Xanthan	2	60	4.5	0.9872	15	1.2

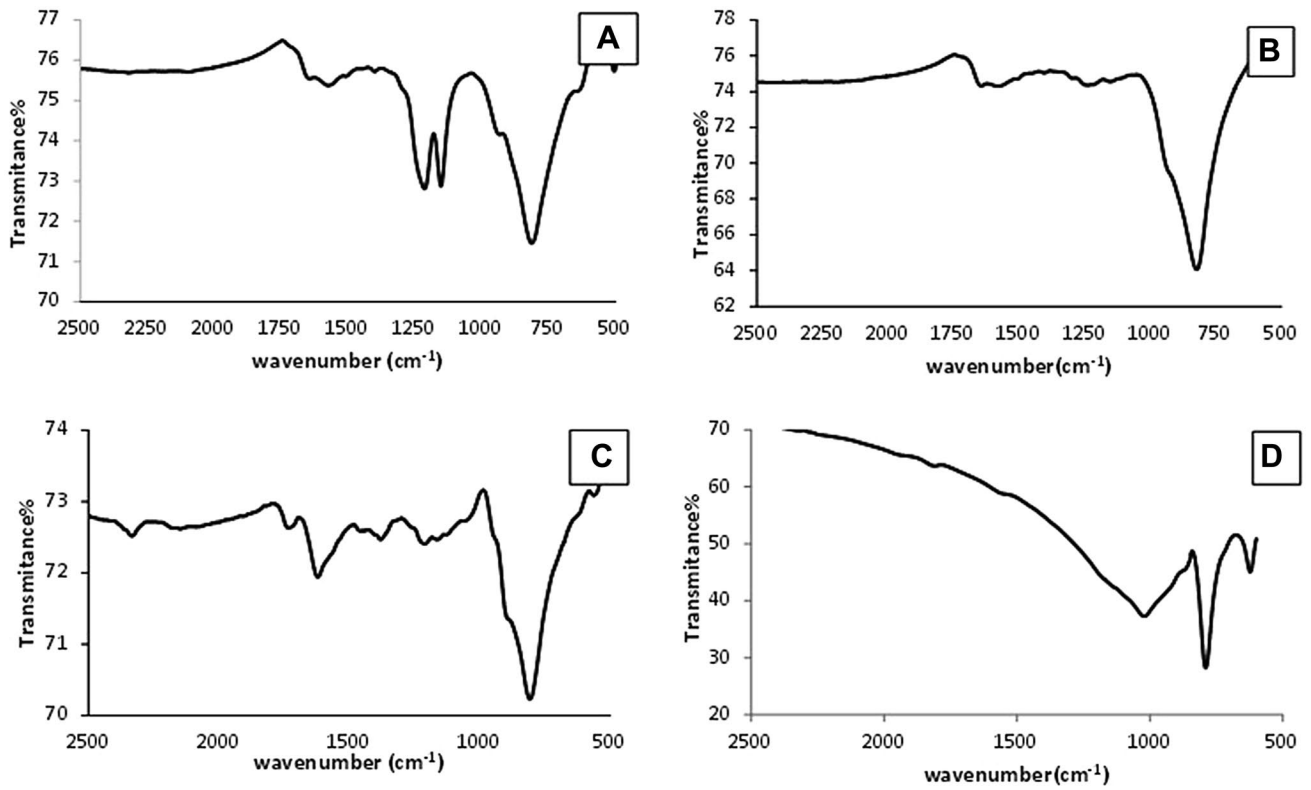

Fig. 1 FTIR spectra of obtained SiC samples: GG (**a**), TG (**b**), AG (**c**), and XG (**d**)

was performed with bio-SiC/MoO_3 catalysts for oxidation of model fuel using H_2O_2 as the oxidant.

Materials and methods

Xanthan gum (MW > 2,000,000; viscosity = 1200–1600), Arabic gum (MW = 250,000–1,000,000; Viscosity = 300), guar gum (MW ~ 250,000; viscosity = 2500–3500), and tragacanth gum (MW ~ 840,000; viscosity = 2000–4000) were prepared naturally and used after purification. (The gums were solved in water, and the insoluble materials were removed by filtration). Tetraethylorthosilicate (Merck) and ethanol (Merck) were used for preparing the silica precursor. Gels pH reduction occurs with acetic acid (Merck). Magnesium powder (0.06–0.3 μm), hydrochloric acid (37%) and hydrofluoric acid (40%), *n*-octane, dodecane, dibenzothiophene, hydrogen peroxide (30%), acetonitrile, and MoO_3 were purchased from Merck.

The SEM images were taken from Tescan, VEGA3 Scanning electron microscope. Infrared spectra (FTIR) were recorded by a Bruker, Vector spectrometer. Bruker, Senterra

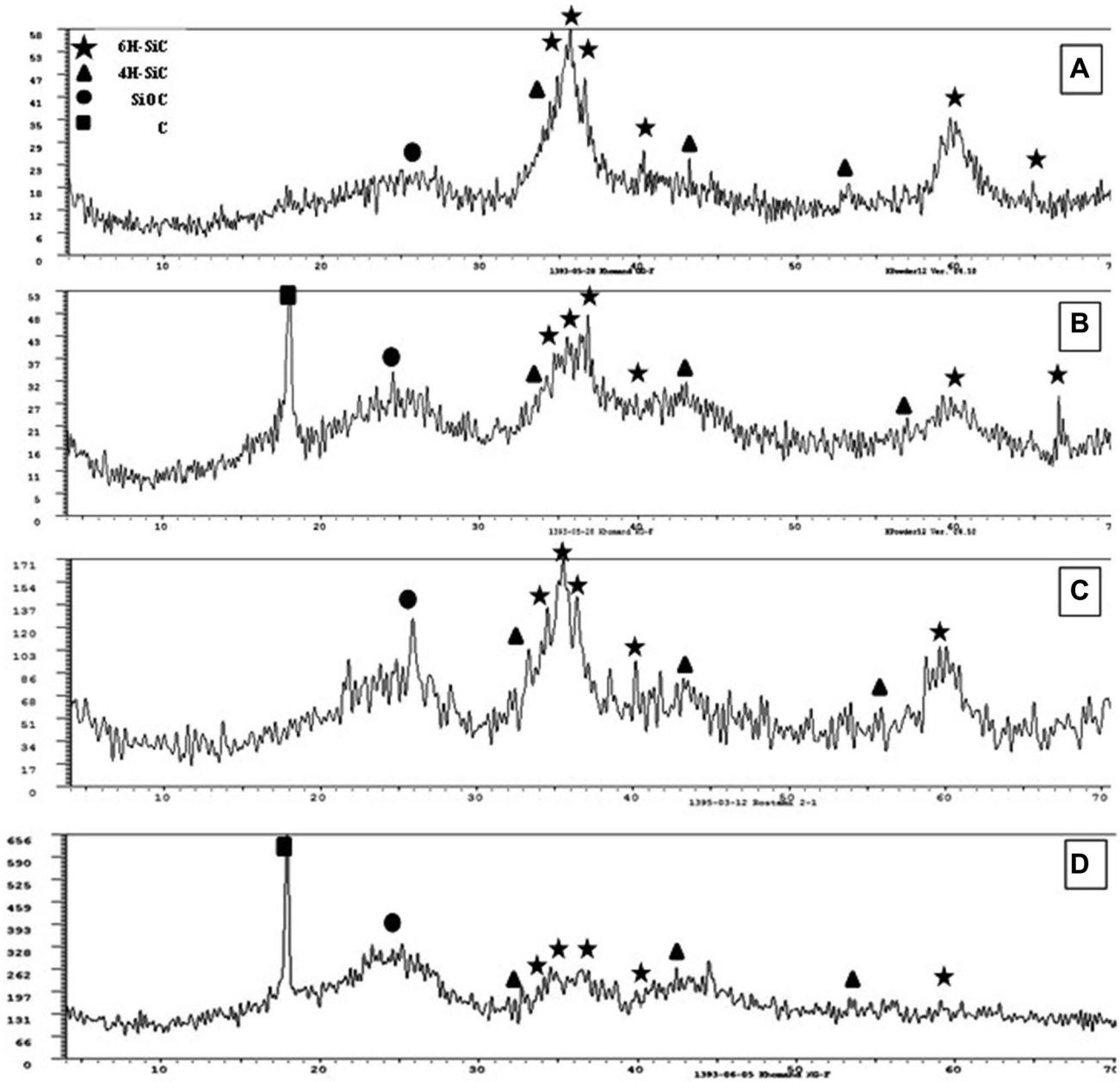

Fig. 2 XRD patterns of obtained SiC samples: GG (**a**), TG (**b**), AG (**c**), and XG (**d**)

micro-Raman instrument was used to record the Raman spectra using a 785-nm laser wavelength. X-ray diffraction (XRD) patterns was used to identify the crystalline phases by using Bruker Axs, D8 Advance, filtered CuK_{α} radiation ($\lambda = 1.54060$ Å). N_2 adsorption/desorption isotherms and pore volume distributions were obtained on the Belsorp mini

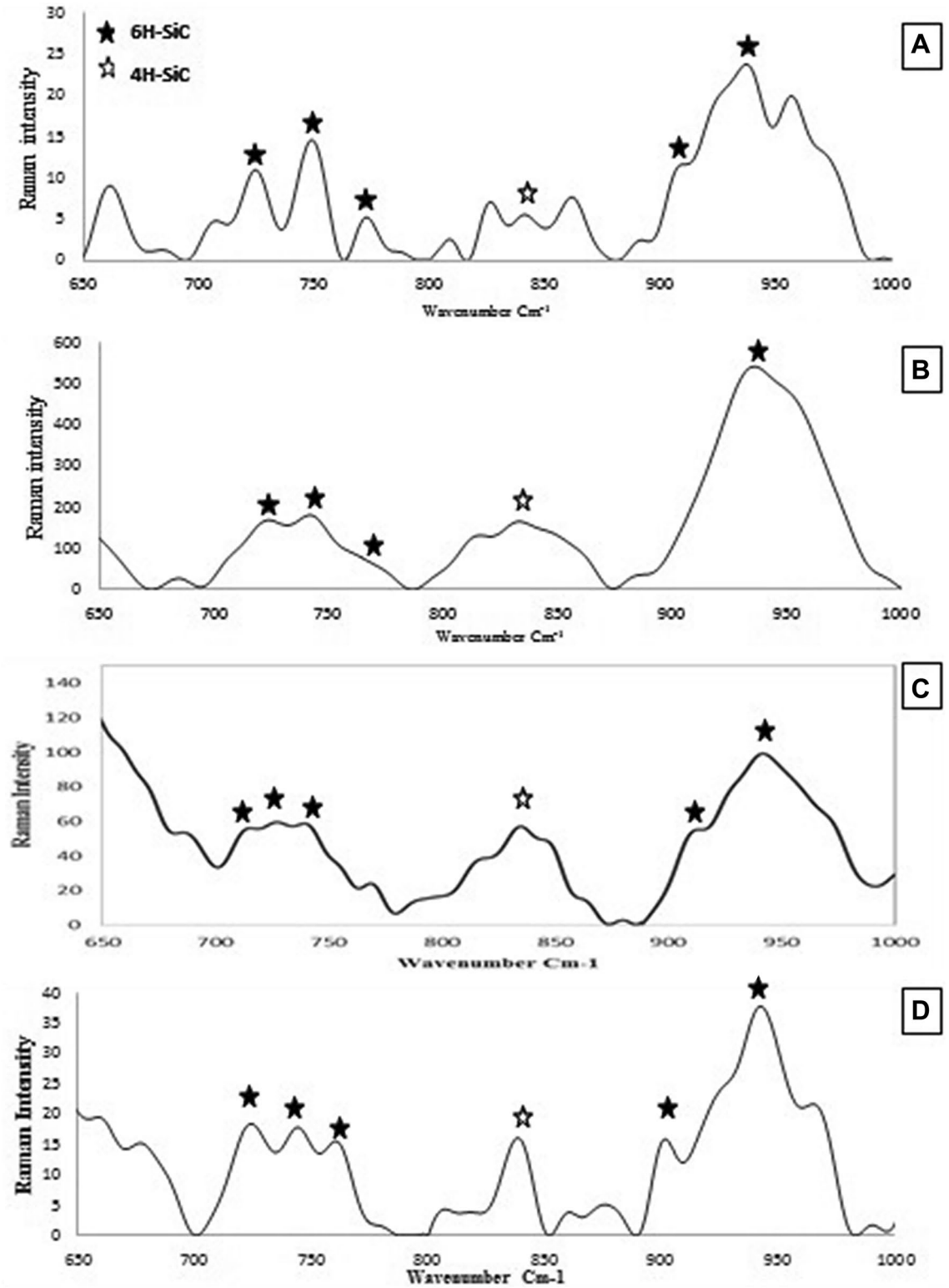

Fig. 3 Raman spectra of obtained SiC samples: GG (**a**), TG (**b**), AG (**c**), and XG (**d**)

instrument. Gas chromatography (GC) was used to investigate the catalytic tests (Faraz Gostar, TG 2552).

Precursors preparation

Gums were prepared in a same way and used as carbon precursors. 2–10 g of gums was dispersed well in a certain volume of distilled water and stirred in a boiling bath for 2 h (Table 1). When the obtained gels cool down to room temperature, they were used as carbon precursors.

Then, silica precursor was prepared using tetraethylorthosilicate (TEOS) according to the previous literature (Moser 1996). TEOS, water, and ethanol were mixed together under mild stirring for 1 h at the ratio of 6:4:3. After the mixture was homogenized, it was used as silica precursor to syntheses the porous silicon carbide materials.

Synthesis of porous silicon carbides

Porous SiCs were prepared by mixing the silica and carbon precursors according to Table 1. The mixtures were homogenized using ultrasonic, and acetic acid solution was added until the resulting mixtures had a pH of 4–5 (Table 1). The mixtures were then put in an oven at 60 °C for 8 h and subsequently at 90 °C for another 8 h. Then, the dried mixtures were carbonized under Ar atmosphere at 750 °C for 1 h. After that, the obtained SiO_2/C composites were mixed well with magnesium powder in the SiO_2: Mg molar ratio of 1:2 and put in a furnace at 700 °C for 6 h (5 °C/min) in argon atmosphere. The obtained porous SiCs were cooled to room temperature and then immersed in a 2 M HCl solution for 24 h to remove the magnesium oxide. Finally, the samples were put in a 2 M HF solution for 24 h to remove the unreacted silica. At last, the samples were washed with water and ethanol, and dried at 40 °C in a vacuum oven for 4 h. The synthesized SiC was denominated as GG, TG, XG, and AG

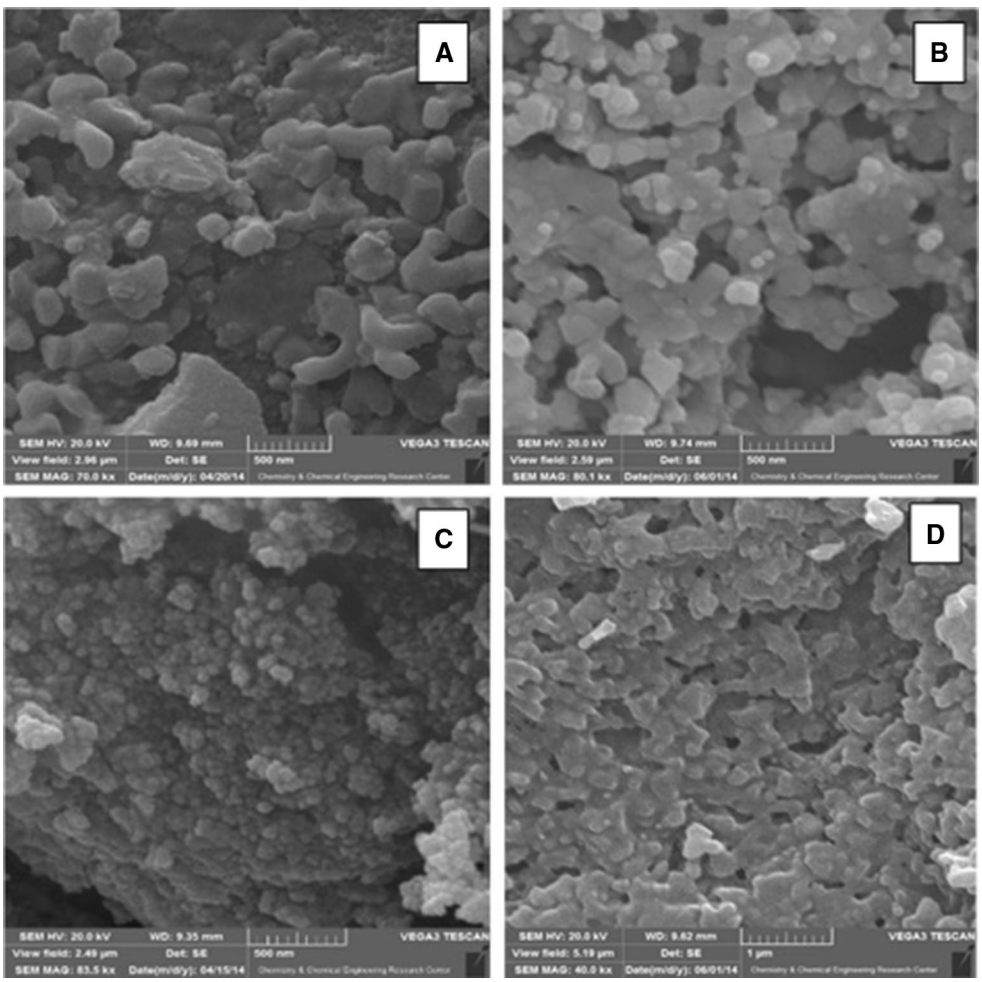

Fig. 4 SEM images of obtained SiC samples without ultrasonic: GG (**a**), TG (**b**), AG (**c**), and XG (**d**)

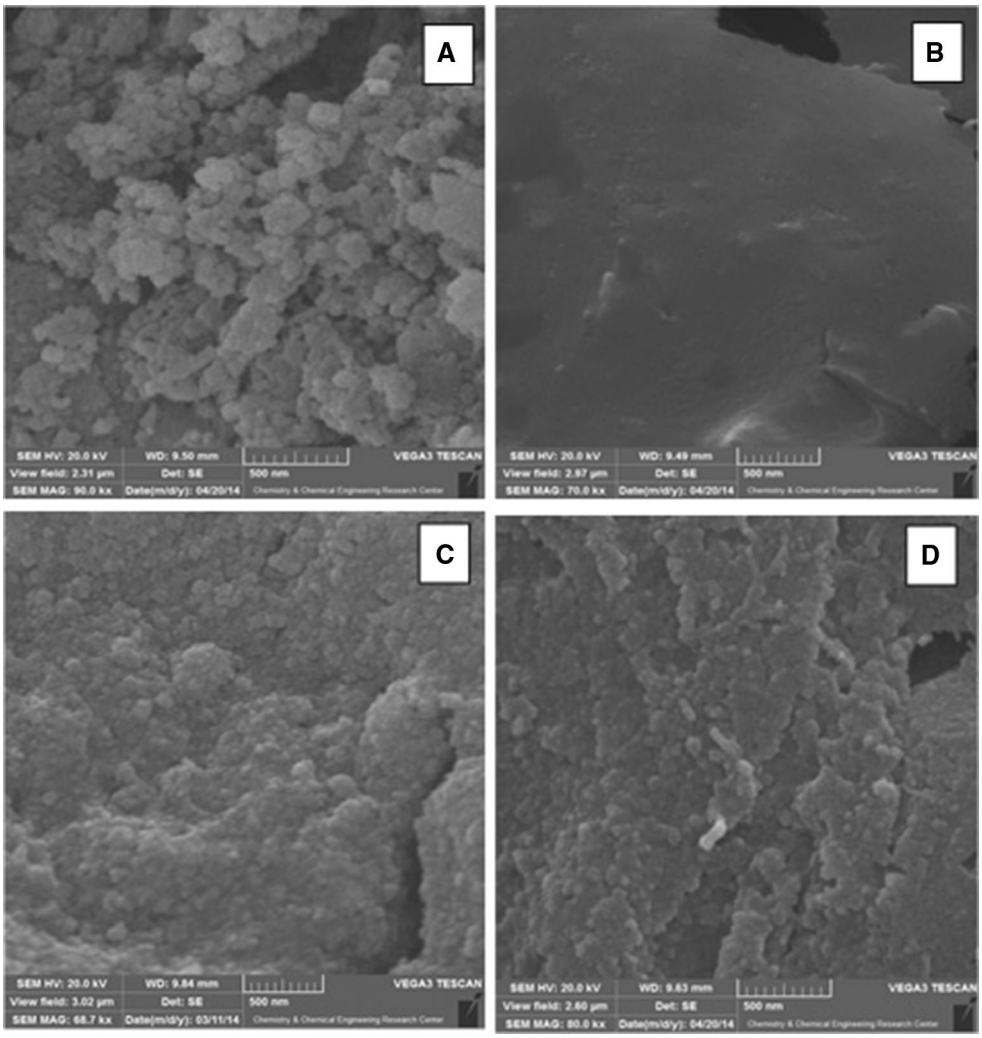

Fig. 5 SEM images of obtained SiC samples under ultrasonic: GG (**a**), TG (**b**), AG (**c**), and XG (d)

corresponding to the guar, tragacanth, xanthan, and Arabic gum templates, respectively.

Preparation of MoO_3/SiC Catalysts

The preparation of these catalysts was carried out in two-stage reaction. In the first stage, active molybdenum oxide precursor (MoO_5) was prepared from molybdenum oxide (VI). 0.72 g MoO_3 was poured in a 50-ml round bottom flask and 5 ml of hydrogen peroxide 30% was added under the temperature of 40 °C for 48 h. The system was stirred until a clear yellow solution was obtained. In the second stage of the reaction, 100 mg of synthesized silicon carbides was added to MoO_5 solution. The obtained products were filtered and washed until the unreacted molybdenum oxide was completely removed. Then, product was placed in the oven to dry for 6 h at 70 °C. The obtained catalyst was tested in the model fuel oxidation reaction.

Catalytic experiments

To prepare the model fuel, 500 ppm of dibenzothiophene (DBT) was dissolved in *n*-octane. 4 ml of model fuel, 10 mg of synthesized catalyst, and 2 ml acetonitrile as extractive solvent were added to a reactor. Dodecane was added to reaction mixture as internal standard and stirred for 5 min. Then, 2 ml of H_2O_2 was introduced. The reaction was taken under stirring at 40 °C. The oil phase was withdrawn in each 20-min period and injected to GC to determine the DBT conversion.

Results and discussion

In order to study the structure of SiC powders, FTIR analysis was used. FTIR spectra of prepared SiC nanostructures are reported in Fig. 1. The vibrations of Si–C bonds appeared at

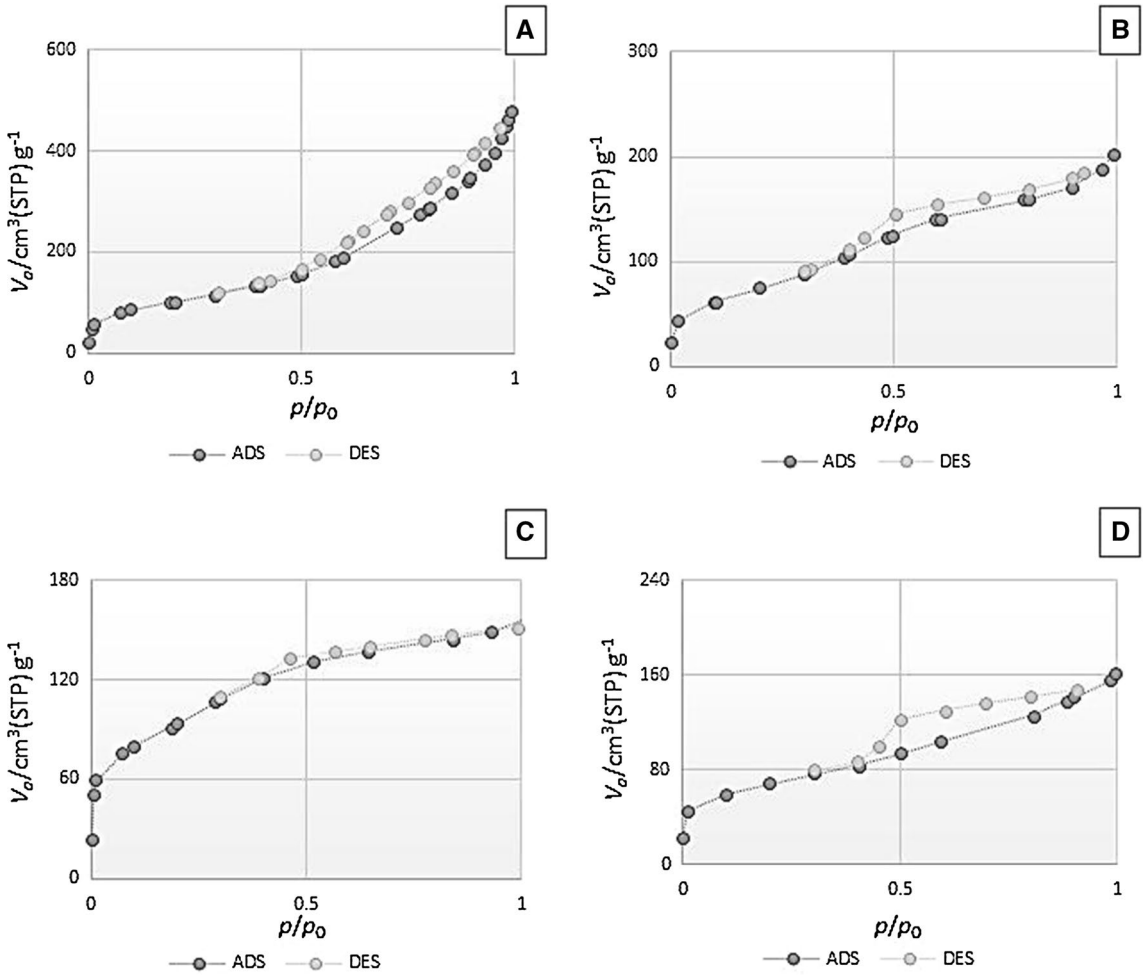

Fig. 6 N_2 adsorption and desorption isotherms of obtained SiC samples: GG (**a**), TG (**b**), AG (**c**), and XG (**d**)

816, 814, 795, and 789 cm^{-1} for GG, TG, AG, and XG samples, respectively. The absorptions observed in 1092, 1159, 1059, and 1100 cm^{-1} are assigned to Si–O–C vibrations in GG, TG, AG, and XG samples, respectively. As shown in Fig. 1, there was a little difference in the Si–C bonds of the prepared SiCs due to the difference in the structures of the gum precursors.

XRD analysis was used to identify the crystal structures of SiC nanostructures. Figure 2 shows the XRD patterns of the prepared SiCs with different gums. The XRD analysis approved the different polymorphs of SiC (6H and 4H). The diffraction peaks at 33.8°, 35.68°, 38.1°, 40.8°, 60.08°, and 65.67° can be assigned as 6H–SiC hexagonal structure (JCPDS#29-1128), indexed as the (101), (102), (103), (104), (110), and (109) reflections, and the diffraction peaks at 33.5°, 34.77°, 35.68°, 38.1°, 42.8°, 57.3°, 60.06°, and 65.7° can be indexed as the (100), (101), (004), (102), (103), (105), (110), and (106) reflections of 4H–SiC hexagonal structure (JCPDS#29-1127). No evidence for the presence of Mg_2Si and Mg_2SiO_4 was observed in patterns, which shows good purification of samples via acid washing.

Raman scattering efficiency for SiC due to the strong covalent chemical bonds is relatively more (Nakashima et al. 2003), and we can easily find useful information such as species, disturbance or structural damage, the network strain, and contaminant movement from this method (Choyke et al. 1997, 2004). Figure 3 shows the Raman scattering spectra of the synthesized SiC samples. In Fig. 3, several vibrations and shoulders were distinguished that were confirmed the presence of mixture of polytypes. The vibrations at about 769, 746, and 722 cm^{-1} correspond to the TO modes of hexagonal structure of SiC (Nakashima and Harima 1997; Bechelany et al. 2007). These vibrations that can be seen for all of synthesized substances were shifted to the lower frequencies than the corresponding bulk material (797, 789, and 767 cm^{-1}). The LO bonds can be seen at 935 and 899 cm^{-1} region. These modes are shifted to lower frequencies compared to bulk material (965 and 889 cm^{-1}).

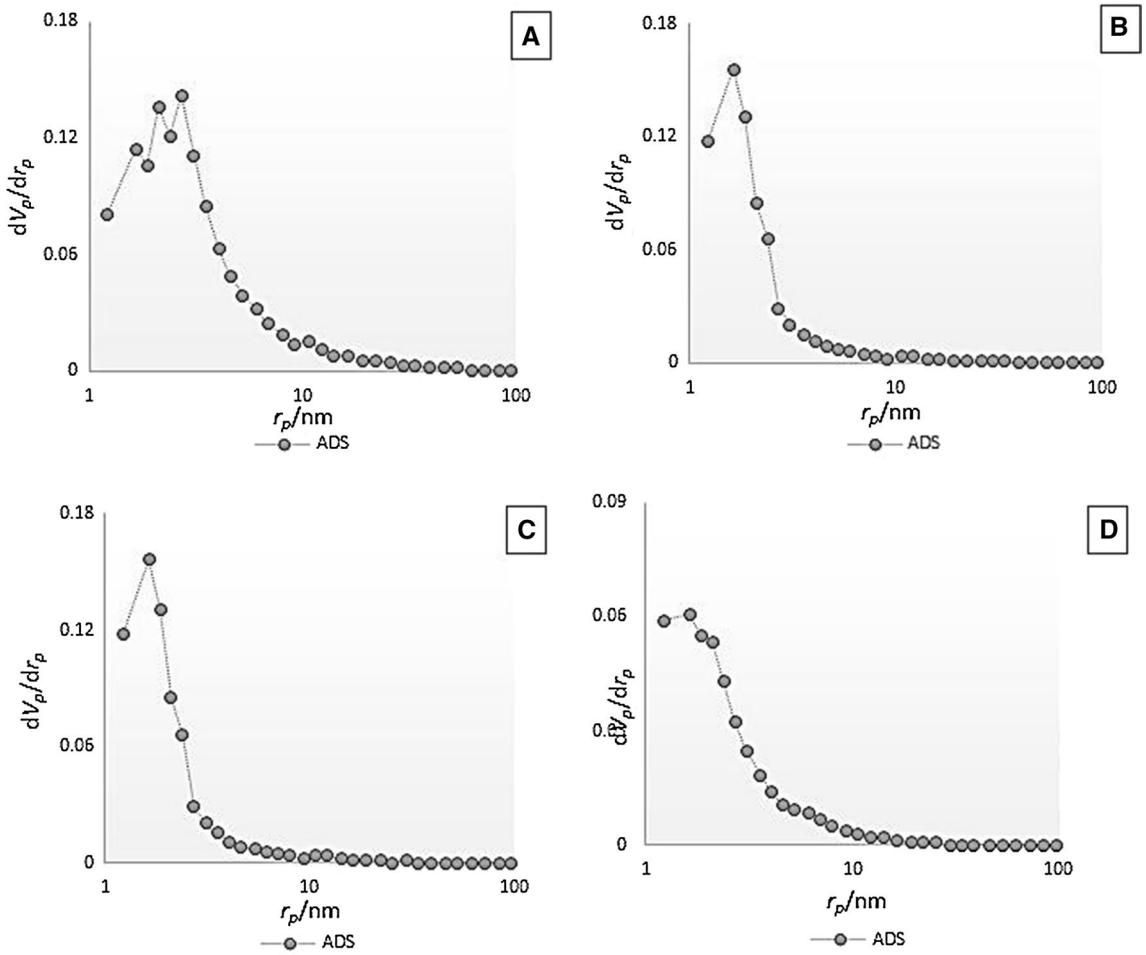

Fig. 7 Pore size distribution plots of obtained SiC samples: GG (**a**), TG (**b**), AG (**c**), and XG (**d**)

Between these two main vibrations, a vibration at 838 cm^{-1} can also be distinguished corresponding to the LO mode of 4H–SiC. Also, several papers that report the vibrations around 800–900 cm^{-1} have shown the structural defects of SiC which often were not observed for materials with a ten times larger diameter (Fig. 3).

Figure 4 shows the SEM micrographs of prepared SiC samples. It was observed in SiC compounds that the gums as the carbon skeleton play a supporting role during reduction procedure and the morphology of final products is varied by changing the structure of carbon precursors.

Figure 5 shows the morphology of synthesized SiC samples with using ultrasonic. Comparing the SEM morphologies shown in Fig. 4 and 5, it is concluded that ultrasonic can make more uniform products with higher surface area.

The mesoporosity of the SiC nanostructures was determined by the N_2 adsorption/desorption measurements (Fig. 6). The synthesized SiC materials exhibit the type-IV isotherm that is the characteristic of mesoporous products. The specific surface area of samples was calculated, for GG, TG, AG, and XG samples, to be 368.22, 278.94, 336.31, and 273.17 m^2/g, respectively. The pore size distribution analysis was studied by BJH method and indicated that the TG, AG, and XG samples have narrow pore size distributions at about 2 nm (Fig. 7). The porosity texture of GG sample is different from others, the mean pore size increases, and two peaks appears around 3–5 nm in the pore size distribution.

Figure 8 shows the morphology of synthesized SiC/MoO_3 catalysts. The images show that the molybdenum oxide particles are immobilized on the surface of silicon carbide samples.

As shown in Fig. 9, the amount of molybdenum oxide is different in SiC samples. This observation can be explained by different morphology and surface area of SiC supports.

The catalytic activity of the synthesized SiC/MoO_3 catalysts was evaluated in the oxidative desulfurization of model fuel. It is observed that sulfone was the only product in the oxidation of DBT by using these catalysts. Figure 10 shows

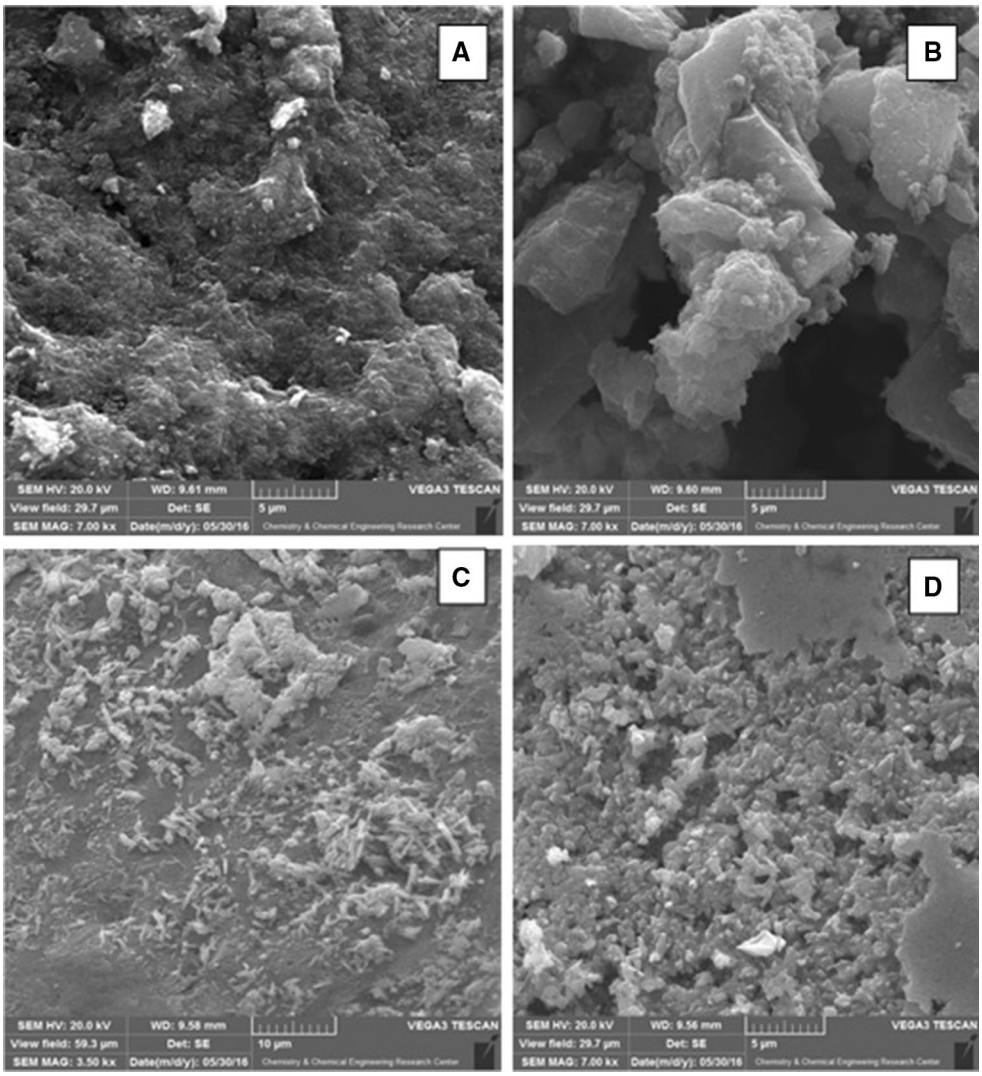

Fig. 8 SEM images of obtained MoO_3/SiC catalysts: GG (**a**), TG (**b**), AG (**c**), and XG (**d**)

the relationships between the sulfur removal efficiency and reaction time for four prepared catalysts at the same condition. This figure shows the effect of SiC support with different nanostructures on the sulfur elimination. The percentage of sulfur elimination from AG, XG, GG, and KG catalysts was 99, 98, 94, and 93%, respectively. The oxidation activity of catalysts was increased by increasing the amount of molybdenum oxide on the surface of SiC supports (Fig. 9). It is obvious that catalytic data can be exactly related to SiC structures (porosity and morphology) that are obtained from their biopolymer precursors.

Results show that the catalytic properties of SiC supports are superior to many of the previously reported for different MoO_3 catalysts in ODS reaction (Table 2). The infinite structure, defects, and also suitable porosity of synthesized bio-SiCs caused the increase in catalytic performance.

To demonstrate the selectivity of these catalysts, the oxidation of model fuel containing different thiophenic derivatives was performed. For this purpose, BT, DBT, and 4,6-DMDBT were used for preparing the model fuel at reported optimal condition (Fig. 11). According to the catalytic data, the best results were obtained for the oxidation of DBT by all the catalysts.

Also, the reusability of catalysts was tested by performing the five series of experiments using the reacted catalysts. The used catalysts were filtered, washed with acetonitrile several times, dried, and then used in another catalytic run. The results showed clearly that only a little loss of catalytic activity was observed even after five runs (Fig. 12).

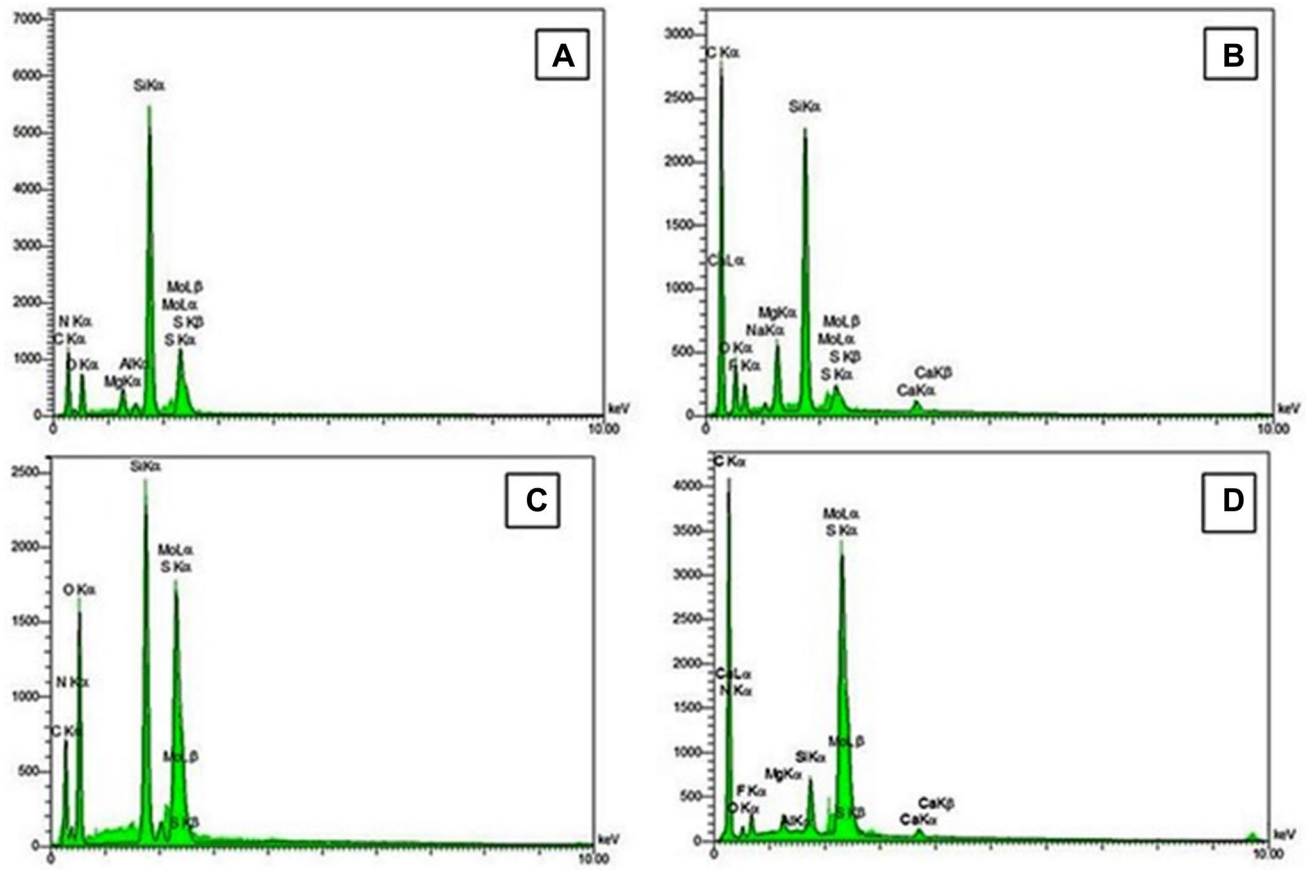

Fig. 9 EDX graphs of obtained MoO_3/SiC catalysts: GG (**a**), TG (**b**), AG (**c**), and XG (**d**)

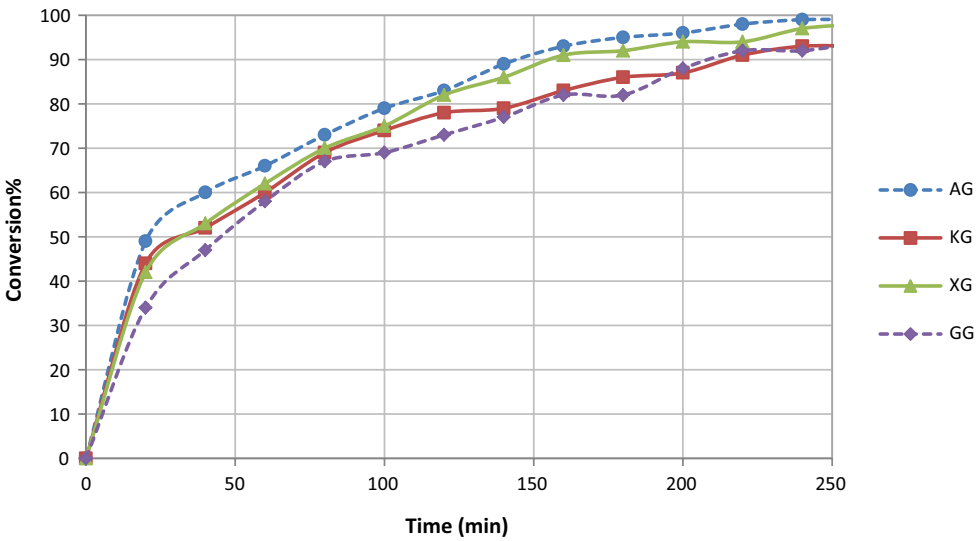

Fig. 10 Comparative study of the oxidation of DBT over SiC/MoO_3 catalysts. Reaction conditions: 4 ml of model fuel (500 ppm), 10 mg of synthesized catalysts, 2 ml acetonitrile, and 2 ml of H_2O_2, 40 °C

Conclusion

In conclusion, we have demonstrated a cost-effective and environmentally friendly strategy to the synthesis of SiC nanostructures from biopolymers as both template and reactant using magnesiothermic method at a relatively low temperature at 700 °C. SEM images of samples indicated that the difference in carbon structures (gums) changes the structure of SiC product. XRD and Raman results showed

Table 2 Comparison of catalytic activities of SiC/MoO_3 catalysts prepared here with other catalyst supports in ODS reaction

Catalyst	Oxidant	Conversion%	References
Mo^{6+}/Al_2O_3	TBHP	90	Bakar et al. (2015)
MoO_3/Al_2O_3	TBHP	84	Prasad et al. (2008)
MoO_3/Magnesia–Al_2O_3	TBHP	12	Prasad et al. (2008)
MoO_3/SiO_2–Al_2O_3	TBHP	95	Prasad et al. (2008)
Fe–MoO_3/Al_2O_3	TBHP	80	Abdullah et al. (2015)
Ca/MoO_3/Al_2O_3	H_2O_2	89.9	Jin et al. (2017)
MoO_3/pseudoboehmite	H_2O_2	97	Cedeno-Caero and Alvarez-Amparan (2014)
MoO_3–CeO_2–SiO_2	CHP	97	Zhang et al. (2009)
MoO_3/SiO_2	CHP	91	Zhang et al. (2009)
Mo_2C/N-doped SiC composite	H_2O_2	99.6	Afsharpour and Rostami Amraee (2017)
MoO_3/SiC (AG)	H_2O_2	99	This article
MoO_3/SiC (XG)	H_2O_2	98	This article
MoO_3/SiC (GG)	H_2O_2	94	This article
MoO_3/SiC (KG)	H_2O_2	93	This article

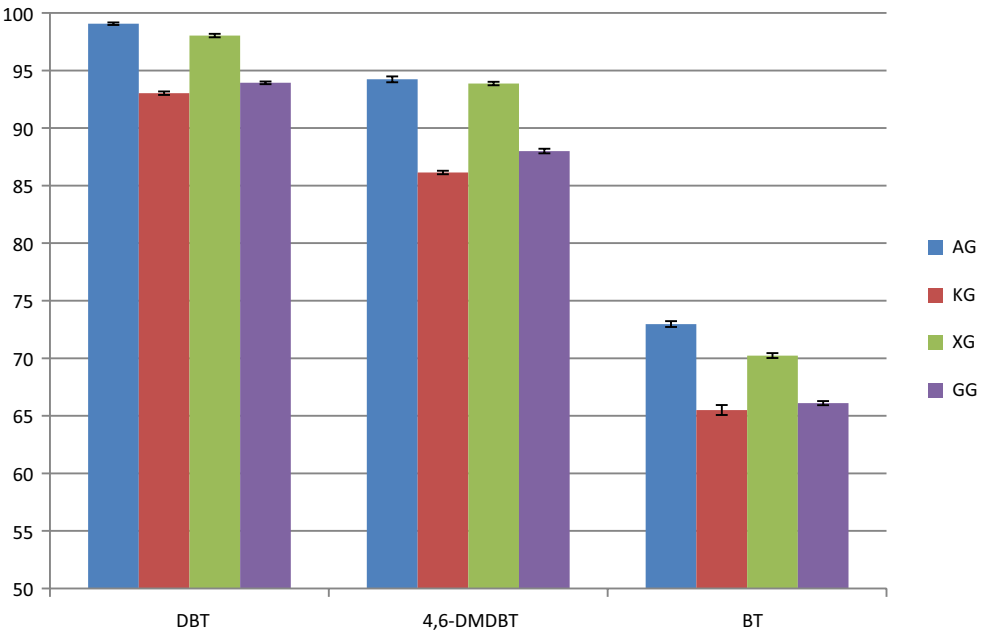

Fig. 11 Oxidation of model fuel of BT, DBT, and 4,6-DMDBT (1:1:1) at optimized condition: 4 ml of model fuel (500 ppm), 10 mg of synthesized catalysts, 2 ml acetonitrile, and 2 ml of H_2O_2, 40 °C (all of the catalytic experiments were triplicated)

the hexagonal structure of obtained SiC that is produced generally in higher temperature. Also, by reducing the synthesis temperature in magnesiothermic method, porous SiC nanostructure was reserved well, and the N_2 adsorption/desorption isotherms approved the mesoporosity structures of SiC samples. Finally, it was observed that the natural biopolymers play an important role in determining the final structure and properties of the SiC products. Also, the results of catalytic tests show the molybdenum oxide catalyst made from silicon carbide supports has high efficiency in the oxidative desulfurization reaction and removal of sulfur compounds from model fuel to obtain ultra-low sulfur fuel (99, 98, 94, and 93% conversion for SiCs produced from Arabic, xanthan, guar, and tragacanth, respectively).

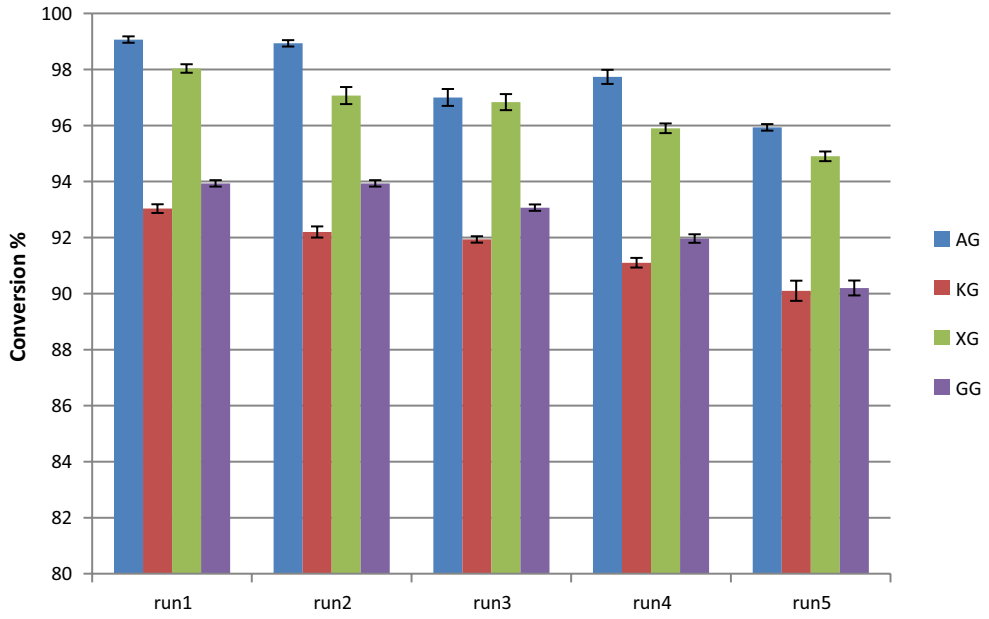

Fig. 12 Recovery of SiC/MoO_3 catalysts after 5 runs at optimized condition (all of the catalytic experiments were triplicated)

Acknowledgements Support for this investigation by Chemistry and Chemical Engineering Research Center of Iran is gratefully acknowledged.

References

Abdullah WNW, Bakar WAWA, Ali R, Embong Z (2015) Oxidative desulfurization of commercial diesel catalyzed by tert-butyl hydroperoxide polymolybdate on alumina: optimization by Box–Behnken design. Clean Technol Environ Policy 17:433–441

Afsharpour M, Rostami Amraee A (2017) Synthesis of bio-inspired N-doped SiC and investigation of its synergetic effects on Mo catalysts in oxidative desulfurization reaction. Mol Catal 436:285–293

Aristov VY, Urbanik G, Kummer K, Vyalikh DV, Molodtsova OV, Preobrajenski AB, Zakharov AA, Hess C, Hanke T, Buchner B (2010) Graphene synthesis on cubic SiC/Si wafers. Perspectives for mass production of graphene-based electronic devices. Nano Lett 10:992–995

Bakar WAWA, Ali R, Kadir AAA, Mokhtar WNAW (2015) The role of molybdenum oxide based catalysts on oxidative desulfurization of diesel fuel. Mod Chem Appl 3:1000150

Bechelany M, Brioude A, Cornu D, Ferro G, Miele P (2007) A Raman spectroscopy study of individual SiC nanowires. Adv Funct Mater 17:939–943

Campos-Martin JM, Capel-Sanchez MC, Perez-Presas P, Fierro JLG (2010) Oxidative processes of desulfurization of liquid fuels. J Chem Technol Biotechol 85:879–890

Cedeno-Caero L, Alvarez-Amparan MA (2014) Performance of molybdenum oxide in spent hydrodesulfurization catalysts applied on the oxidative desulfurization process of dibenzothiophene compounds. React Kinet Mech Catal 113:115–131

Chica A, Corma A, Dómine ME (2006) Catalytic oxidative desulfurization (ODS) of diesel fuel on a continuous fixed-bed reactor. J Catal 242:299–308

Choyke WJ, Matsunami H, Pensl G (1997) Silicon carbide: a review of fundamental questions and applications to current device technology. Akademie Verlag, Berlin

Choyke WJ, Matsunami H, Pensl G (2004) Silicon carbide: recent major advances. Springer, Berlin

Daşdelen Z, Yıldız Y, Eriş S, Şen F (2017) Enhanced electrocatalytic activity and durability of Pt nanoparticles decorated on GO-PVP hybride material for methanol oxidation reaction. Appl Catal B Environ 219:511–516

Dasog M, Rachinsky C, Veinot JG (2011) From Si and C encapsulated SiO_2 to SiC: exploring the influence of sol–gel polymer substitution on thermally induced nanocrystal formation. J Mater Chem 21:12422–12427

Dasog M, Smith LF, Purkait TK, Veinot JG (2013) Low temperature synthesis of silicon carbide nanomaterials using a solid-state method. Chem Commun 49:7004–7006

Davis SA, Breulmann M, Rhodes KH, Zhang B, Mann S (2001) Template-directed assembly using nanoparticle building blocks: a nanotectonic approach to organized materials. Chem Mater 13:3218–3226

De Filippis P, Scarsella M (2008) Peroxyformic acid formation: a kinetic study. Ind Eng Chem Res 47:973–975

Eddy Jr C, Gaskill D (2009) Silicon carbide as a platform for power electronics, DTIC Document.

Garcia-Gutierrez JL, Fuentes GA, Hernández-Terán ME, Garcia P, Murrieta-Guevara F, Jiménez-Cruz F (2008) Ultra-deep oxidative desulfurization of diesel fuel by the Mo/Al_2O_3–H_2O_2 system: The effect of system parameters on catalytic activity. Appl Catal A Gen 334:366–373

Haw KG, Bakar WAWA, Ali R, Chong JF, Kadir AAA (2010) Catalytic oxidative desulfurization of diesel utilizing hydrogen peroxide and functionalized-activated carbon in a biphasic diesel–acetonitrile system. Fuel Process Technol 91:1105–1112

He L, Li H, Zhu W, Guo J, Jiang X, Lu J, Yan Y (2008) Deep oxidative desulfurization of fuels using peroxophosphomolybdate catalysts in ionic liquids. Ind Eng Chem Res 47:6890–6895

Henderson EJ, Kelly JA, Veinot JG (2009) Influence of HSiO sol – gel polymer structure and composition on the size and luminescent properties of silicon nanocrystals. Chem Mater 21:5426–5434

Jayakumar R, Nagahama H, Furuike T, Tamura H (2008) Synthesis of phosphorylated chitosan by novel method and its characterization. Int J Biol Macromol 42:335–339

Jiang Z, Ma Y, Zhou Y, Hu S, Han C, Pei C (2013) Facile fabrication of three-dimensional mesoporous Si/SiC composites via one-step magnesiothermic reduction at relative low temperature. Mater Res Bull 48:4139–4145

Jin W, Tian Y, Wang G, Zeng D, Xu Q, Cui J (2017) Ultra-deep oxidative desulfurization of fuel with H_2O_2 catalyzed by molybdenum oxide supported on alumina modified by Ca^{2+}. RSC Adv 7:48208–48213

Ledoux MJ, Pham-Huu C (2001) Silicon carbide: a novel catalyst support for heterogeneous catalysis. Cattech 5:226–246

Lewis MA (1992) The effects of mixtures and other environmental modifying factors on the toxicities of surfactants to freshwater and marine life. Water Res 26:1013–1023

Magnani G, Sico G, Brentari A, Fabbri P (2014) Solid-state pressureless sintering of silicon carbide below 2000 °C. J Eur Ceram Soc 34:4095–4098

Mélinon P, Masenelli B, Tournus F, Perez A (2007) Playing with carbon and silicon at the nanoscale. Nat Mater 6:479–490

Mjalli FS, Ahmed OU, Al-Wahaibi T, Al-Wahaibi Y, AlNashef IM (2014) Deep oxidative desulfurization of liquid fuels. Rev Chem Eng 30:337–378

Moser WR (1996) Advanced catalysts and nanostructured materials: modern synthetic methods. Academic Press, Cambridge

Nakashima SI, Harima H (1997) Raman investigation of SiC polytypes. Phys Status Solidi (a) 162:39–64

Nakashima S, Higashihira M, Maeda K, Tanaka H (2003) Raman scattering characterization of polytype in silicon carbide ceramics: comparison with X-ray diffraction. J Am Ceram Soc 86:823–829

Prabaharan M, Jayakumar R (2009) Chitosan-graft-β-cyclodextrin scaffolds with controlled drug release capability for tissue engineering applications. Int J Boil Macromol 44:320–325

Prasad VVDN, Jeong KE, Chae HJ, Kim CU, Jeong SY (2008) Oxidative desulfurization of 4,6-dimethyl dibenzothiophene and light cycle oil over supported molybdenum oxide catalysts. Catal Commun 9:1966–1969

Rao JB, Kush D, Bhargava N (2012) Production and characterization of nano structured silicon carbide by high energy ball milling. J Miner Mater Charact Eng 11:529–532

Sanchez C, Julian B, Belleville P, Popall M (2005) Applications of hybrid organic–inorganic nanocomposites. J Mater Chem 15:3559–3592

Selby H, Wynne W (1973) Agar. Industrial gums. Academic Press, New York, pp 29–48

Sen B, Kuzu S, Demir E, Akocak S, Sen F (2017) Highly monodisperse RuCo nanoparticles decorated on functionalized multiwalled carbon nanotube with the highest observed catalytic activity in the dehydrogenation of dimethylamine–borane. Int J Hydrogen Energy 42:23299–23306

Tian Y, Yao Y, Zhi Y, Yan L, Lu Sh (2015) Combined extraction-oxidation system for oxidative desulfurization (ODS) of a model fuel. Energy Fuel 29:618–625

Wen L, Ma Y, Dai B, Zhou Y, Liu J, Pei C (2013) Preparation and dielectric properties of SiC nanowires self-sacrificially templated by carbonated bacterial cellulose. Mater Res Bull 48:687–690

Wright NG, Horsfall AB, Vassilevski K (2008) Prospects for SiC electronics and sensors. Mater Today 11:16–21

Yang W, Araki H, Tang C, Thaveethavorn S, Kohyama A, Suzuki H, Noda T (2005) Single-crystal SiC Nanowires with a thin carbon coating for stronger and tougher ceramic composites. Adv Mater 17:1519–1523

Yildiz Y, Okyay TO, Sen B, Gezer B, Kuzu S, Savk A, Demir E, Dasdelen Z, Sert H, Sen F (2017) Highly monodisperse pt/rh nanoparticles confined in the graphene oxide for highly efficient and reusable sorbents for methylene blue removal from aqueous solutions. Chem Select 2:697–701

Zhang J, Bai X, Li X, Wang A, Ma X (2009) Preparation of MoO_3–CeO_2–SiO_2 oxidative desulfurization catalysts by a sol–gel procedure. Chin J Catal 30:1017–1021

Zhao H, Nagy KL, Waples JS, Vance GF (2000) Surfactant-templated mesoporous silicate materials as sorbents for organic pollutants in water. Environ Sci Technol 34:4822–4827

Zhao B, Zhang H, Tao H, Tan Z, Jiao Z, Wu M (2011) Low temperature synthesis of mesoporous silicon carbide via magnesiothermic reduction. Mater Lett 65:1552–1555